Characterization of iron-sensitive R2*-qMRI in the Substantia Nigra in Psychotic Spectrum Disorders

Paul Wirsching, Sophie Fromm, Anna Schädlich, Lara Wieland, Ralph Buchert, Stefan Hetzer, Jakob Kaminski, Florian Schlagenhauf

Characterization of iron-sensitive R2*-qMRI in the Substantia Nigra in Psychotic Spectrum Disorders

Paul Wirsching[1], Sophie Fromm[1,2,3,4], Anna Schädlich[1], Lara Wieland[1,2,3], Ralph Buchert[4], Stefan Hetzer[1,6], Jakob Kaminski[1] and Florian Schlagenhauf[1,2]

1 Department of Psychiatry and Neuroscience | CCM, Charité-Universitätsmedizin Berlin, corporate member of Freie Universität Berlin, Humboldt-Universität zu Berlin, and Berlin Institute of Health CCM, Berlin, German

2 Charité – Universitätsmedizin Berlin, Einstein Center for Neurosciences Berlin, Berlin, Germany

3 Bernstein Center for Computational Neuroscience, Berlin, Germany

4 Department of Psychology, Humboldt-Universität zu Berlin, Germany

5 Department of Nuclear Medicine, University Medical Center Hamburg-Eppendorf (*UKE*), Hamburg, Germany

6 Berlin Center for Advanced Neuroimaging, Charité-Universitätsmedizin Berlin, Berlin, Germany

Corresponding author: Paul Wirsching (paul.wirsching@charite.de)

Short title: Iron-sensitive MRI in psychosis

Keywords: Neuromelanin, psychosis, schizophrenia, biomarker, quantitative MRI, dopamine-proxy

Introduction

Psychotic spectrum disorders (PSD) represent a relevant proportion of psychiatric patients in hospitals and outpatient settings and affect up to 1 -3 % of the general population (Perälä et al., 2007). The diagnostic process of psychosis spectrum disorder is based exclusively on clinical examination and the patient's medical history (Jauhar et al., 2022), since no routine biomarkers for psychosis are available (Abi-Dargham et al., 2023).

Excessive dopaminergic signaling in striatal F-DOPA-PET is a well-described neural alteration relevant for the pathophysiology of psychotic symptoms (Howes et al., 2012; Mccutcheon et al., 2018; Jauhar et al., 2022; Abi-Dargham et al., 2023). While providing crucial in-vivo information on the dopaminergic homeostasis, PET's potential as a clinical routine diagnostic tool remains limited due to its high cost, radiation exposure, and long acquisition times, which are not feasible in the clinical setting for diagnosing patients with acute psychotic disorders.

Neuromelanin-sensitive MRI (NM-MRI) of the substantia nigra (SN) has emerged as a potential in-vivo marker for dopaminergic aberration (Cassidy et al., 2019; Wieland et al., 2021). This technique exploits the

unique magnetic properties of neuromelanin (NM), a byproduct of dopamine synthesis that accumulates as protein-iron-complexes in dopaminergic neurons. NM is a granular pigment that accumulates with oxidation of cytosolic catecholamines, such as dopamine or epinephrine (Zecca et al., 2003), typically found in regions such as the substantia nigra (SN), the locus coeruleus (LC) or the ventral tegmental area (VTA). The oxidation is promoted by ferric iron that reacts with cytosolic proteins, resulting in non-degradable NM-iron protein complexes. These complexes have an idiosyncratic dark colour and paramagnetic properties that perturb the magnetic field and can thus be imaged with MR-techniques (Sulzer et al., 2018). NM in the SN accumulates with age (Zecca et al., 2003; Sulzer et al., 2018) and is decreased in patients with Parkinson's diesease (e.g. (Sasaki et al., 2006), where the loss of dopaminergic neurons is central to pathogenesis.

In patients with schizophrenia, increased NM signals in the SN are a well reported finding (Wieland et al., 2021; Ueno et al., 2022). A recent study on NM in the SN of psychotic patients succeeded to perform out-of-sample prediction of psychosis severity based on NM-MRI of the SN (Wengler et al., 2024), further highlighting NM's potential in clinical application.

While a promising tool in research, however, NM-MRI's long scan times might complicate the routine application of in acute psychosis, where patients are often agitated or anxious. Furthermore, different methods to calculate the signal-noise-ratio to a reference region lower comparability between studies. Addressing these limitations, we here evaluate a more readily available alternative MRI parameter: the effective transverse relaxation rate (R2* = 1/T2*) which characterizes signal dephasing caused by local field distortions and was shown to reflect the total iron content in dopaminergic neurons (Brammerloh et al., 2021). The multi-parameter mapping (MPM) approach (Weiskopf et al., 2013) allows not only to estimate R2* from a rapid MRI scan (< 7 min) but provides a set of four complementary physical tissue parameters which are linked to the microstructural tissue composition (Cooper et al., 2020). Therefore, MPM has the potential to overcome NM-MRIs disadvantages to investigate the complex microstructural changes of cerebral tissue associated with psychotic disorders. Regarding psychosis, the R2* parameter is only reported in two studies in first-episode psychosis (Xu et al., 2021; García Saborit et al., 2023). While García Saborit et al. (2023) did not detect group differences in R2* parameter in the SN, Xu et al. (2021) report reduced R2* parameter in the SN of patients with a first psychotic episode.

In the present preprint publication we report a preliminary characterization of the R2* signal as well as three other qMRI sequences in the substantia nigra of a sample of psychosis spectrum disorder patients and healthy control participants. Furthermore, we investigate correlation of the R2* parameter with symptom burden, demographic factors, and report its association with striatal dopamine synthesis capacity in a healthy PET subsample to support its relevance to dopaminergic signaling.

Methods

Participants

Fourty healthy participants were recruited via flyers, online advertisement, email- and messenger lists. Healthy participants had no medical, neurological and current lifetime psychiatric disorder assessed with the Structured Clinical Interview for Diagnostic and Statistical Manual of Mental Disorders (First et al., 2015). Fourty-eight patients were recruited from the Charité Hospital, Psychiatry and Psychotherapy Department as well as from affiliated psychiatric hospitals, day clinics or outpatient units. Patients with psychotic spectrum disorders (PSD) met ICD-10 criteria of the schizophrenia spectrum (F.2x) or substance-induced psychosis (F10.5-F19.5). All participants were required to be proficient of the German language, aged 18-60 years and to provide written informed consent prior to participation. Currently active substance abuse was an exclusion criterion.

The study was approved by the ethics committee of Charitè - Universitätsmedizin Berlin and was carried out in accordance with the Declaration of Helsinki. The data was collected over a period of ~4 years (2019 - 2023) within a larger study. Eligibility was assessed by research assistants within the team and psychiatric assessment was conducted by trained researchers. Participants were financially reimbursed with 8.00 € per hour and received an additional reward within another study part.

Assessment of psychopathology and cognitive function

Psychiatric assessment of psychotic symptoms was conducted using the Positive and Negative Syndrome Scale (PANSS) (Kay et al., 1987). Other measured variables including demographic variables, gender and total illness duration were assessed during the interview routine.

MRI acquisition and processing

MRI scans were acquired on a 3T MR Scanner (Magnetom Prisma, Siemens Healthineers, Erlangen, Germany) equipped with a 64-channel receive radio frequency head-neck coil. The MPM scan with 1.6 mm isotropic resolution was comprised of three different 3D-multi-echo fast low-angle shot (FLASH) gradient-echo acquisitions. MR sequence parameters were: repetition time TR = 37ms, flip angle FA = 6◦ for MT-weighted images with a Gaussian off- resonance RF pulse (500◦, 10 ms, 1,200 Hz off-resonance, 192 Hz bandwidth) prior to non-selective excitation; TR = 18 ms, FA = 4◦ and 25◦ for PD-weighted images and T1-weighted images. The field of view was 224 x 256mm2 (matrix-size of 140× 160) with isotropic resolution of 1.60 mm, and 112 partitions, readout bandwidth 470 Hz/pixel allowing six echoes between 2.46 and 14.78 ms for all three acquisitions. MPM maps of longitudinal relaxation rate (R1 = 1/T1), effective transverse relaxation rate (R2* = 1/T2*), magnetization transfer (MT) and proton density sequences (PD) were generated using the hMRI toolbox (Tabelow et al., 2019) including corrections for transmit RF pulse inhomogeneity and Gibb's ringing according to Cooper et al. (2020). Magnetic resonance imaging (MRI) data were processed and analyzed using the Statistical Parametric Mapping (SPM12) toolbox (Wellcome Trust Centre for Neuroimaging, London, UK) implemented in

MATLAB (MathWorks, Natick, MA, USA). This included the preprocessing steps realignment, normalization to the Montreal Neurological Institute (MNI) space, and for voxel-wise comparisons, smoothing with an isotropic Gaussian kernel of 2 mm. Subsequent statistical analyses (see below) were conducted within the SPM12 framework or in combination with R.

First, VOI-analyses were performed for each sequence. Here, averaged unsmoothed qMRI signal intensities were extracted from a mask of the substantia nigra, obtained from Neurovault, https://neurovault.org/collections/3145/ (Pauli et al., 2018)) for each participant. Extracted parameters were subjected to further statistical analysis with R as outlined below. Additionally, for group-comparisons, a voxel-wise comparison of the R2*-signal intensity between patients with psychosis spectrum disorder and healthy participants was performed on smoothed qMRI-images with age as a covariate.

PET acquisition and processing

In a subgroup of 16 healthy participants, PET scans were performed to measure the dopamine synthesis capacity by the FDOPA utilization rate constant Ki^{cer} (min^{-1}), estimated by the graphical tissue-slope intercept method according to Patlak-Gjedde on a voxel by voxel base. A mask of the cerebellum (without vermis) was created using the WFU Pick-Atlas in SPM 12 and used as a reference. Scans were acquired in a hybrid PET/MRI Siemens 3 T MR-system (Siemens Healthineers, Erlangen, Germany). PET emission data were reconstructed according to an iterative algorithm in 20 frames (3×20 s, 3×1 min, 3×2 min, 3×3 min, 7×5 min, 1×6 min) with an isotropic voxel size of 2 mm. Images were realigned and coregistered, using the unified segmentation approach in SPM, Matlab, resulting in parametric Ki^{cer}maps.

Statistical analyses

Image processing and voxel-wise analysis was carried out using Matlab and the SPM12 package. All further statistical analyses were conducted using R version 4.3.0 (R Core Team, 2024). Linear regression models were applied to investigate the association between R2* and clinical group, age and symptom intensity, derived from PANSS scores. Pearson's correlations were calculated where indicated. In the PET-subgroup of healthy controls, we investigated the association of KI^{cer} values in the striatum with R2* MRI signal intensity in the SN, while including age as a covariate.

Results

Demographic and clinical data

The final sample of PSD subjects included 38 patients diagnosed with paranoid schizophrenia (SCZ), 2 with schizoaffective disorder (SCAD), 1 patient with persistent delusional disorder (DD), 1 with brief

psychotic disorder (BPD), and 6 with Substance induced psychosis (SIP), summarized in Table 1. Psychotic spectrum disorder subjects (PSD) were significantly older than healthy controls (HC) (36.65 ± 9.94 vs 28.98 ± 9.69 years, t=3.66, p = <.001). There was no significant difference in proportion of gender between the groups (X^2 (1, N = 88) = 3.244, p = .071). Regarding symptom severity, the average PANSS total score of patients was 28.52 ± 9.24, average PANSS positive scale was 14.83 ± 5.13, average PANSS negative scale 14.52 ± 6.76 and average PANSS general psychopathology average 28.52 ± 9.24. Patients had an average illness duration of 11.23 (± 9.11) years, The average illness duration (Table 1) was not related to participant age (R-squared = 0.3937, F(1, 46) = 31.52, p < 0.001). Illness duration did not significantly correlate with PANSS scores (PANSS total r = 0.03, p = 0.83, PANSS positive r = -0.048, p = 0.75, PANSS negative r = 0.14, p = 0.35, PANSS psych r = 0.032, p = 0.83).

Table 1 Demographic and clinical data of the sample: HC = Healthy Controls, PSD = psychotic spectrum disorder, SCZ = schizophrenia, SCAD = schizoaffective disorder, DD = delusional disorder, BPD = brief psychotic disorder, SIP = substance induced psychosis, PANSS = positive and negative symptom score.

		HC	PSD	Statistics
n		40	48	
Sex (f/m)		21/19	15/33	
Age (years)		28.98 ± 9.69	36.65 ± 9.94	t=3.81, p= <.01**
Diagnosis (n)			SCZ (20),	
			SCAD (2),	
			DD (1),	
			BPD (1),	
			SIP (6)	
PANSS	Positive symptoms		14.83 ± 5.13	β = -0.40, t(77.98) = -0.97, p = 0.34
	Negative symptoms		14.52 ± 6.76	(β = -0.14, t(85.97) = -0.34, p = 0.74
	Gen. psychopathology		28.52 ± 9.24	β = -0.289, t(43) = -1.20, p = 0.23
Duration of illness (years)			11.23 ± 9.11	

1.1 Characterization of R2* in the substantia nigra

Age-dependent increase in R2-SN specific for PSD subjects*

In a first step, the averaged R2* parameter within an SN mask was probed for association with the subjects age in linear regression analyses for both the PSD and the HC group individually (Figure 1). While there was no significant age-dependent effect of R2* in HC ($F(1, 46) = 1.84$, $R^2 = 0.046$, $p = 0.18$), PSD subjects showed a significant increase of the R2* parameter with age ($F(1, 46) = 8.98$, $R^2 = 0.16$, $p = 0.0044$ **). Adding duration of illness as a covariate, age remained a significant predictor of R2*-SN in PSD, while illness showed a trend-wise positive association with R2*-SN ($F(1, 44) = 4.21$, adj. $R^2 = 0.17$, $p_{age} = 0.0041$ **, $p_{illn.dur} = 0.07$).

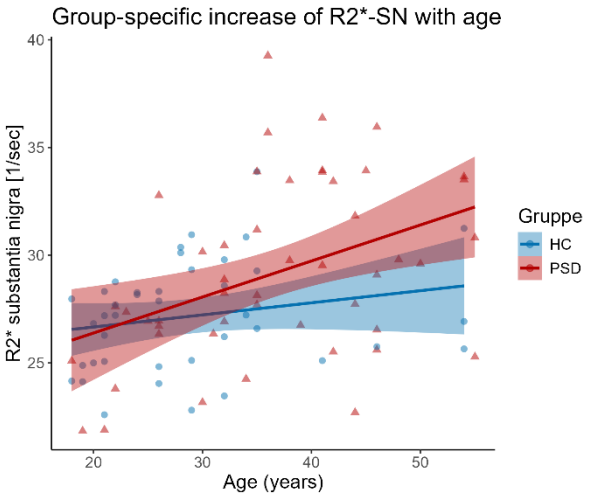

Figure 1: Group-specific and age-dependent increase of the effective transverse relaxation rate R2 in the SN of PSD subjects in a linear regression model. HC ($F(1, 46) = 1.84$, $R^2 = 0.046$, $p = 0.18$), PSD ($F(1, 46) = 8.98$, $R^2 = 0.16$, $p = 0.0044$ **).*

Voxel-wise comparison

Voxel-wise comparisons with age as a covariate identified bilateral clusters in the SN mask with increased signal-intensity in PSD compared to HC, as reported in

Table 2. The left and right clusters included 19 and 24 significant voxels. A 3D-render of the voxels allowed their anatomical localization in the ventral SN (Figure 2 A). The increased mean R2* values within the clusters in PSD compared to HC are depicted in Figure 2 B.

Table 2: Voxel-wise comparison revealed two clusters with statistically significant increase (PSD > HC) in the R2 parameter. The clusters are located in the bilateral SN's and include 19 and 24 voxels respectively. Coordinates refer to MNI coordinate system.*

R2* PSD > HC	**Coordinate [x/y/z]**	**T-value**	**pFWE (peak-level)**	**Number of voxels**
	-9 / -8 / -12	4.36	.004	19
	9 / -11 / -14	4.18	.007	24

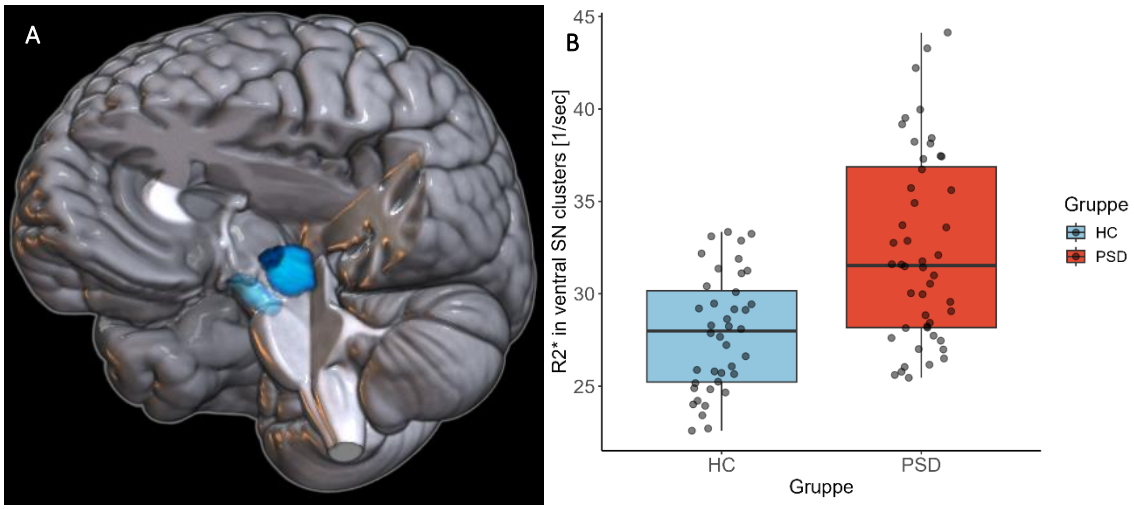

Figure 2: Voxel-wise comparison identified clusters with age-dependent increase of R2 in the ventral SN of patients. A: 3D-render of the significant clusters (dark blue) that exhibit an increased R2*-signal in the SN (light blue) of PSD subjects, while controlling for age. Clusters are overlayed on a standard brain model. B: Increased mean R2* signal within the clusters in PSD compared to HC.*

No significant association of R2 signal with psychotic symptom severity*

Neither PANSS total, PANSS positive, PANSS negative, and PANSS psychopathology (Figure 3, A - D) were significant predictors of R2* (summarized in Table 1). Taken together, symptom severity as measured by the PANSS does not significantly correlate with R2* in the substantia nigra when controlling for age. These results did not change upon analysis of the average values from the significant SN clusters (results not shown).

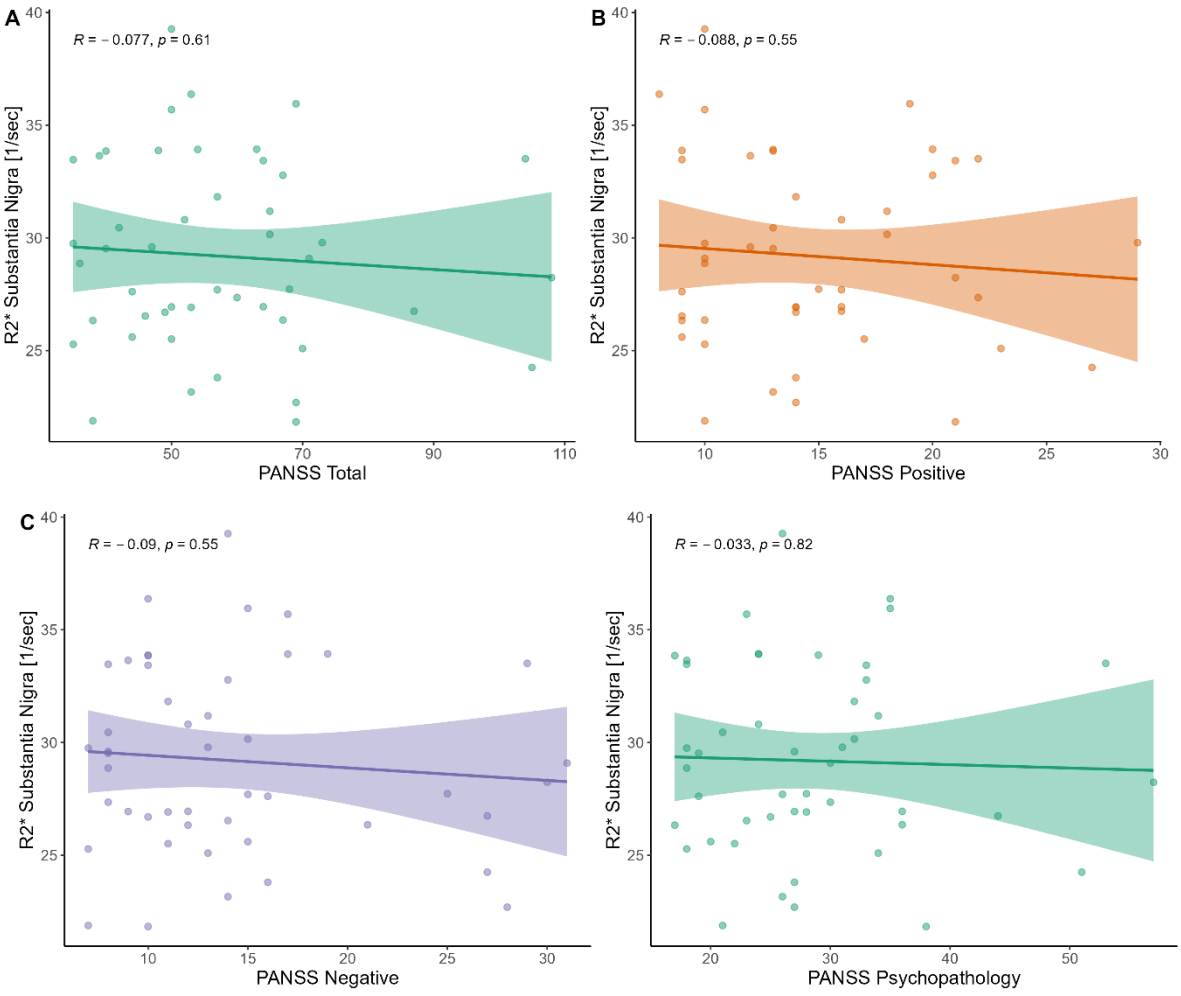

Figure 3: Association of symptom severity with R2 in the SN revealed no significant correlation regarding PANSS total (A), PANSS positive (B), PANSS negative (C), and PANSS psychopathology (D).*

1.2 Negative correlation of R2* intensity in substantia nigra with striatal dopamine synthesis capacity in F-DOPA-PET

In a subgroup of healthy control subjects, we performed 18F-Dopa-PET measurements of striatal KIcer (reflecting the presynaptic dopamine synthesis capacity of midbrain dopaminergic neurons) and tested for an association with R2*-SN. Neither R2*-SN (β = -0.00025, p = 0.55) nor age (β = -0.000083, p = 0.80) significantly predicted KIcer in the striatum. The relationship between R2*-SN and striatal dopamine synthesis capacity did not significantly change with age (β = -0.0000012, p = 0.92).

Despite the lack of significant individual predictors, the overall model was statistically significant (F(3, 12) = 8.82, p = 0.0023 **), accounting for a considerable portion of the variance in KIcer, with an R-squared value of 0.69 and an adjusted R-squared of 0.61 (Figure 4). As such, approximately 61% of the variability in striatal dopamine synthesis capacity can be explained by the model, The residuals of the

linear model, representing the proportion of the correlation that is not explained by age, showed a strong correlation (r = -0.63, t(14) = -3.03, p = 0.009 **).

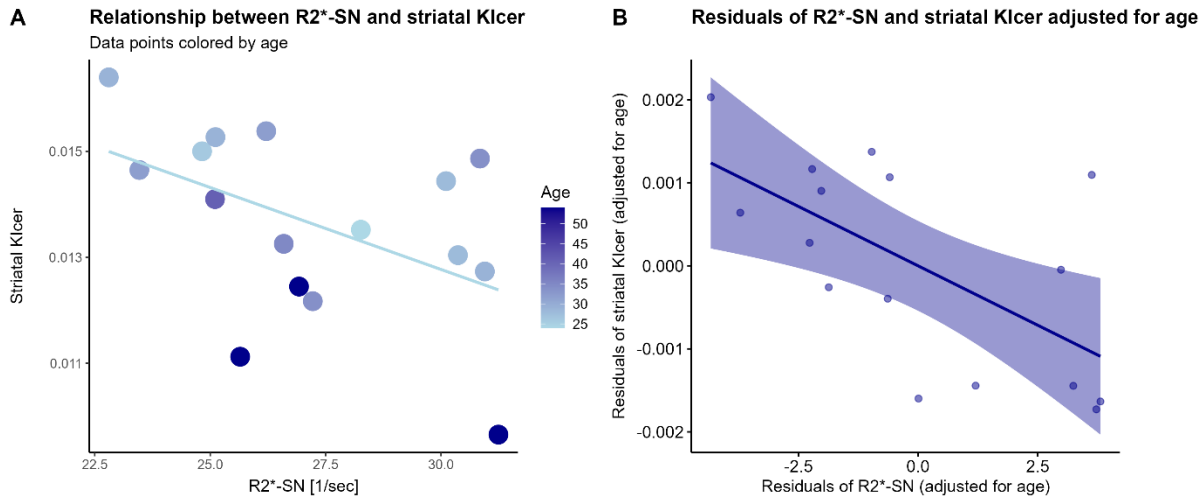

Figure 4: Correlation between R2 in the SN and striatal 18F-Dopa-PET KIcer in a subsample of healthy controls. A: Scatterplot with datapoints colored by age. B: To account for confounding effects of age, the residuals of the linear model were correlated after regressing out age, representing the proportion of the correlation that is not explained by age (r = -0.63, t(14) = -3.03, p = 0.009 **).*

1.3 No group difference in the qMRI sequences R1, PD and MT

As described above, we measured four different quantitative MPM maps (R2*, R1, PD and MT), following previous reports (Cooper et al., 2020). Unlike R2*, average SN-signal intensities of the other sequences did not differ between patients and controls in the longitudinal relaxation rate R1 (0.818 vs 0.810, t(81.30) = 0.90, p = 0.37), the proton density PD (72.71 vs 72.29, t(77.98) = 1.294, p = 0.20), and the magnetization transfer saturation MT (2.982 vs 2.990, t(85.97) = -0.181, p = 0.857) (plotted in Figure 5 A – C).

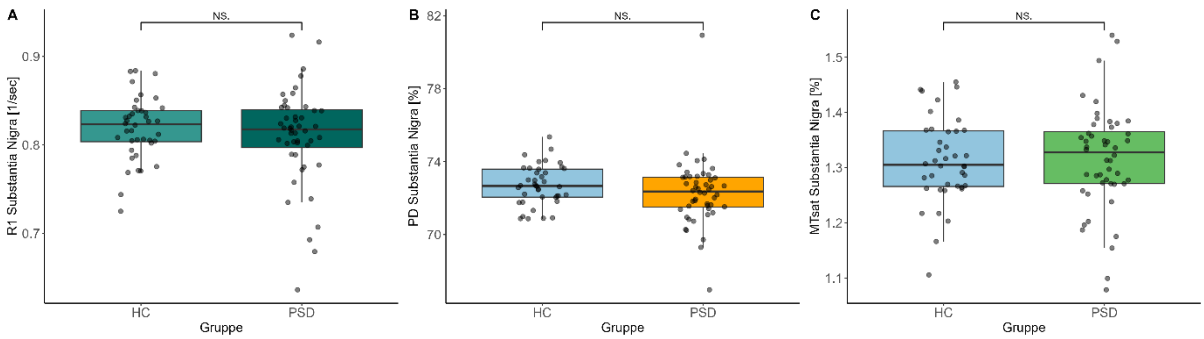

Figure 5: Group-wise comparison of mean signal intensity of three qMRI sequences in the SN revealed no group differences between PSD and HC regarding the longitudinal relaxation rate R1 (A), the proton density PD(B), and the magnetization transfer saturation MT (C).

Discussion

The study reported explores the quantitative iron-sensitive MRI map R2* (effective transverse relaxation rate) as a potential in-vivo markers for dopaminergic aberration similar to neuromelanin sequences. NM-MRI leverages on the unique magnetic properties of the dopamine synthesis byproduct neuromelanin (NM) that accumulates as protein-iron-complexes in dopaminergic neurons (Cassidy et al., 2019; Horga et al., 2021; Wengler et al., 2024). A meta-analysis of NM-MRI-studies is reported in (Wieland et al., 2021; Ueno et al., 2022), where increased NM-MRI-CNR in psychotic patients is a robust finding. Recently even an association with symptom severity was reported (Wengler et al., 2024), supporting the role of NM-MRI as a potential marker in psychosis. However, the long scan times and CNR-calculations hinder routine application and comparability of results between sites. Multi parameter mapping (MPM) qMRI-sequences overcome those challenges by providing absolute measures in a short scan time (<7 min) (Cooper et al., 2020).

In this study, we investigated the potential of the transverse relaxation rate (R2*) and other quantitative MRI maps to differentiate between cases and controls in psychosis spectrum disorders (PSD).

Age-related increase of R2 signal in SN of PSD subjects*

The subjects age showed to be a strong confounder of R2* in our sample, especially, since the PSD group was significantly older than controls. This finding is in line with existing literature (Treit et al., 2021). Still, we were able to detect two clusters in the ventral SN of PSD subjects with increased R2* parapmeter compared to HC in voxel-wise comparisons accounting for age effects. These results underscore the potential of the R2* map in the investigation of neurobiological alterations in psychosis. However, the non-significant relationship between R2*-sigcl and age highlights the nuanced relationship between these variables and underscores the need for further research.

Existing literature on R2*, and more general, brain-iron-sensitive MRI in psychotic patients is scarce and yields conflicting results. While Xu et al. (Xu et al., 2021) reported a decrease in R2* in the SN of patients with a first psychotic episode, and García Saborit et al. did not detect group differences in R2*- in the SN of first episode patients (García Saborit et al., 2023), Ravanfar et al found an overall increased brain iron signature in the SN of chronic schizophrenia patients (Ravanfar et al., 2022). These results might reflect the strong age-dependent effect on R2* that we report in our results and might suggest a significantly increased accumulation of neuromelanin-iron-complexes only to happen over several years of psychosis.

No significant association between R2 and symptom severity in our sample.*

The lack of a significant correlation between symptom severity, as measured by the Positive and Negative Syndrome Scale (PANSS), and R2* aligns with the notion that NM accumulation - and by extension, changes in R2* - occurs over an extended period. Therefore, these changes may not directly reflect acute psychotic states but rather longer-term neurobiological processes.

Complex association of midbrain R2 and dopamine synthesis capacity derived from FDOPA-PET*

We observed a negative correlation between R2*-SN and striatal KIcer in a subsample of healthy controls. Both measures were correlated with age and correlation between R2*-SN and striatal KIcer remained significant also when removing age effects from both measures. These observations hints at underlying complexities in the determinants of KIcer that extend beyond the measurable impacts of iron-sensitive R2* measures in the midbrain, highlighting the multifaceted nature of factors influencing dopamine synthesis capacity in the human striatum.

qMRI signals R1, PD, and MT in substantia nigra unaltered in PSD

No group differences were observed in the qMRI sequences of R1, PD, and MT, suggesting that the neuroanatomical changes of SN in psychosis are specifically measured by R2*. This specificity supports the potential of the MRI map R2* over other qMRI sequences in distinguishing between PSD and HC groups, particularly in older individuals.

Limitations

While providing novel insights into the neurobiological underpinnings of psychosis spectrum disorders, our study has several limitations that warrant consideration. First, the healthy control group was not ideally matched to the patient group in terms of age and gender, especially since age proved a strong confounder of the R2* parameter. Furthermore, the subsample for PET imaging is relatively small and was only performed in a subsample of healthy controls and not in PSD subjects, which limits the clinical implications of the measurements.

Additionally, the contributing effects determining the R2* parameter are not completely understood. While we primarily focused on the iron detecting ability in the context of neuromelanin complexes in this study, iron is involved in multiple processes in the brain (see e.g. (Ravanfar et al., 2022)), namely the formation of myelin. Further studies should aim for a direct intra-sample comparison of R2* with established sequences such as NM-MRI.

Outlook

In conclusion, our study advances the understanding of the neurobiological alterations associated with psychosis, emphasizing the complex interplay between alterations in the R2* parameter, and dopamine synthesis capacity. Future research should aim to untangle these relationships further, incorporating longitudinal designs and larger sample sizes to validate the potential of R2* as a neurobiological marker for psychosis spectrum disorders.

References

Abi-Dargham A, Moeller SJ, Ali F, DeLorenzo C, Domschke K, Horga G, Jutla A, Kotov R, Paulus MP, Rubio JM, Sanacora G, Veenstra-VanderWeele J, Krystal JH. 2023. Candidate biomarkers in psychiatric disorders: state of the field. World Psychiatry, 22(2):236–262 DOI: 10.1002/wps.21078.

Brammerloh M, Morawski M, Friedrich I, Reinert T, Lange C, Pelicon P, Vavpetič P, Jankuhn S, Jäger C, Alkemade A, Balesar R, Pine K, Gavriilidis F, Trampel R, Reimer E, Arendt T, Weiskopf N, Kirilina E. 2021. Measuring the iron content of dopaminergic neurons in substantia nigra with MRI relaxometry. Neuroimage, 239 DOI: 10.1016/J.NEUROIMAGE.2021.118255.

Cassidy CM, Zucca FA, Girgis RR, Baker SC, Weinstein JJ, Sharp ME, Bellei C, Valmadre A, Vanegas N, Kegeles LS, Brucato G, Kang UJ, Sulzer D, Zecca L, Abi-Dargham A, Horga G. 2019. Neuromelanin-sensitive MRI as a noninvasive proxy measure of dopamine function in the human brain. Proc Natl Acad Sci U S A, 116(11):5108–5117 DOI: 10.1073/PNAS.1807983116/-/DCSUPPLEMENTAL.

Cooper G, Hirsch S, Scheel M, Brandt AU, Paul F, Finke C, Boehm-Sturm P, Hetzer S. 2020. Quantitative Multi-Parameter Mapping Optimized for the Clinical Routine. Front Neurosci, 14 DOI: 10.3389/fnins.2020.611194.

García Saborit M, Jara A, Muñoz N, Milovic C, Tepper A, Alliende LM, Mena C, Iruretagoyena B, Ramirez-Mahaluf JP, Diaz C, Nachar R, Castañeda CP, González A, Undurraga J, Crossley N, Tejos C. 2023. Quantitative Susceptibility Mapping MRI in Deep-Brain Nuclei in First-Episode Psychosis. Schizophr Bull, 49(5):1355–1363 DOI: 10.1093/SCHBUL/SBAD041.

Horga G, Wengler K, Cassidy CM. 2021. Neuromelanin-sensitive MRI as a proxy marker for catecholamine function in psychiatry. JAMA psychiatry, 78(7):788 DOI: 10.1001/JAMAPSYCHIATRY.2021.0927.

Howes OD, Kambeitz J, Kim E, Stahl D, Slifstein M, Abi-Dargham A, Kapur S. 2012. The Nature of Dopamine Dysfunction in Schizophrenia and What This Means for Treatment: Meta-analysis of Imaging Studies. Arch Gen Psychiatry, 69(8):776–786 DOI: 10.1001/ARCHGENPSYCHIATRY.2012.169.

Jauhar S, Johnstone M, McKenna PJ. 2022. Schizophrenia. Lancet, 399(10323):473–486 DOI: 10.1016/S0140-6736(21)01730-X.

Mccutcheon R, Beck K, Jauhar S, Howes OD. 2018. Defining the Locus of Dopaminergic Dysfunction in Schizophrenia: A Meta-analysis and Test of the Mesolimbic Hypothesis. Schizophr Bull, 44(6):1301–1311 DOI: 10.1093/schbul/sbx180.

Pauli WM, Nili AN, Michael Tyszka J. 2018. A high-resolution probabilistic in vivo atlas of human subcortical brain nuclei. Sci Data 2018 51, 5(1):1–13 DOI: 10.1038/sdata.2018.63.

Perälä J, Suvisaari J, Saarni SI, Kuoppasalmi K, Isometsä E, Pirkola S, Partonen T, Tuulio-Henriksson A, Hintikka J, Kieseppä T, Härkänen T, Koskinen S, Lönnqvist J. 2007. Lifetime prevalence of psychotic and bipolar I disorders in a general population. Arch Gen Psychiatry, 64(1):19–28 DOI: 10.1001/ARCHPSYC.64.1.19.

R Core Team. 2024. R: A Language and Environment for Statistical Computing. [accessed: 03/09/2024] URL: https://www.r-project.org/.

Ravanfar P, Syeda WT, Jayaram M, Rushmore RJ, Moffat B, Lin AP, Lyall AE, Merritt AH, Yaghmaie N, Laskaris L, Luza S, Opazo CM, Liberg B, Chakravarty MM, Devenyi GA, Desmond P, Cropley VL, Makris N, Shenton ME, Bush AI, Velakoulis D, Pantelis C. 2022. In Vivo 7-Tesla MRI Investigation of Brain Iron and Its Metabolic Correlates in Chronic Schizophrenia. Schizophrenia, 8(1) DOI: 10.1038/s41537-022-00293-1.

Sasaki M, Shibata E, Tohyama K, Takahashi J, Otsuka K, Tsuchiya K, Takahashi S, Ehara S, Terayama Y, Sakai A. 2006. Neuromelanin magnetic resonance imaging of locus ceruleus and substantia nigra in Parkinson's disease. Neuroreport, 17(11):1215–1218 DOI: 10.1097/01.WNR.0000227984.84927.A7.

Sulzer D, Cassidy C, Horga G, Kang UJ, Fahn S, Casella L, Pezzoli G, Langley J, Hu XP, Zucca FA, Isaias IU, Zecca L. 2018. Neuromelanin detection by magnetic resonance imaging (MRI) and its promise as a biomarker for Parkinson's disease. npj Park Dis 2018 41, 4(1):1–13 DOI: 10.1038/s41531-018-0047-3.

Tabelow K, Balteau E, Ashburner J, Callaghan MF, Draganski B, Helms G, Kherif F, Leutritz T, Lutti A, Phillips C, Reimer E, Ruthotto L, Seif M, Weiskopf N, Ziegler G, Mohammadi S. 2019. hMRI - A toolbox for quantitative MRI in neuroscience and clinical research. Neuroimage, 194:191–210 DOI: 10.1016/J.NEUROIMAGE.2019.01.029.

Treit S, Naji N, Seres P, Rickard J, Stolz E, Wilman AH, Beaulieu C. 2021. R2* and quantitative susceptibility mapping in deep gray matter of 498 healthy controls from 5 to 90 years. Hum Brain Mapp, 42(14):4597–4610 DOI: 10.1002/HBM.25569.

Ueno F, Iwata Y, Nakajima S, Caravaggio F, Rubio JM, Horga G, Cassidy CM, Torres-Carmona E, de Luca V, Tsugawa S, Honda S, Moriguchi S, Noda Y, Gerretsen P, Graff-Guerrero A. 2022. Neuromelanin accumulation in patients with schizophrenia: A systematic review and meta-analysis. Neurosci Biobehav Rev, 132:1205–1213 DOI: 10.1016/J.NEUBIOREV.2021.10.028.

Weiskopf N, Suckling J, Williams G, Correia M. MM, Inkster B, Tait R, Ooi C, Bullmore T. ET, Lutti A. 2013. Quantitative multi-parameter mapping of R1, PD*, MT, and R2* at 3T: a multi-center validation. Front Neurosci, 7(7 JUN) DOI: 10.3389/FNINS.2013.00095.

Wengler K, Baker SC, Velikovskaya A, Fogelson A, Girgis RR, Reyes-Madrigal F, Lee S, de la Fuente-Sandoval C, Ojeil N, Horga G. 2024. Generalizability and Out-of-Sample Predictive Ability of Associations Between Neuromelanin-Sensitive Magnetic Resonance Imaging and Psychosis in Antipsychotic-Free Individuals. JAMA Psychiatry, 81(2):198–208 DOI: 10.1001/JAMAPSYCHIATRY.2023.4305.

Wieland L, Fromm S, Hetzer S, Schlagenhauf F, Kaminski J. 2021. Neuromelanin-Sensitive Magnetic Resonance Imaging in Schizophrenia: A Meta-Analysis of Case-Control Studies. Front Psychiatry, 12 DOI: 10.3389/fpsyt.2021.770282.

Xu M, Guo Y, Cheng Junying, Xue K, Yang M, Song X, Feng Y, Cheng Jingliang. 2021. Brain iron assessment in patients with First-episode schizophrenia using quantitative susceptibility mapping. NeuroImage Clin, 31 DOI: 10.1016/j.nicl.2021.102736.

Zecca L, Zucca FA, Costi P, Tampellini D, Gatti A, Gerlach M, Riederer P, Fariello RG, Ito S, Gallorini M, Sulzer D. 2003. The neuromelanin of human substantia nigra: structure, synthesis and molecular behaviour. J Neural Transm Suppl, (65):145–155 DOI: 10.1007/978-3-7091-0643-3_8.